Available online at www.sciencedirect.com
ScienceDirect
Lithos 97 (2007) 122–139
LITHOS
www.elsevier.com/locate/lithos

A-type magmatism in the Western Lachlan Fold Belt? A study of granites and rhyolites from the Grampians region, Western Victoria

J. Hergt *, J. Woodhead, A. Schofield

School of Earth Sciences, The University of Melbourne, Victoria, 3010, Australia

Received 25 October 2005; accepted 4 December 2006
Available online 15 December 2006

Abstract

The Victoria Valley Batholith, a granite–rhyolite complex of unusual composition, was emplaced in the Grampians–Stavely Zone of western Victoria at 396 Ma. Petrographic and geochemical features of the suite share important similarities with A-type magmas and we propose that they be classified as such. The close association between metaluminous to weakly peraluminous A-types and peralkaline granites within the Victoria Valley suite requires that, at least in some cases, these lithologies should be grouped together as part of a single A-type suite. This relationship is not necessarily a magmatic one as at least some of the peralkaline rocks in this suite appear to be the result of hydrothermal alteration. The Sr, Nd and Hf isotopic compositions of the magmas at the time of their emplacement (0.70459, 0.51220 and 0.28274) are remarkably similar to those of Cambrian mafic to intermediate lithologies calculated at 396 Ma. We suggest that the Victoria Valley suite was produced via the partial melting of basement Cambrian rocks (perhaps similar to diorites associated with the ~495 Ma Bushy Creek pluton to the southeast) and that the magmas subsequently underwent variable fractional crystallisation dominated by hornblende and plagioclase. The oxidation state of the Victoria Valley magmas remains unclear, but is likely to have been higher than that observed in ferroan A-types suggesting that low oxygen fugacity is not an essential pre-requisite for A-type magmatism.

Keywords: A-type; Granite; Isotope geochemistry; Peralkaline; Isochron

1. Introduction

Southeastern Australia provides an unparalleled opportunity to investigate granite petrogenesis. The ~700 km wide Siluro-Devonian Lachlan Fold Belt constitutes one of the largest well-exposed granite terranes in the world, and preserves a wide range in compositions (e.g., White and Chappell, 1988; Chappell and White, 1992). A volumetrically minor group, referred to as A-type granites, has long been recognised as displaying distinctive geochemical characteristics (e.g., Collins et al., 1982; Clemens et al., 1986; Whalen et al., 1987; King et al., 1997), particularly in granites with the lowest silica contents (~65–72% SiO_2; King et al., 2001).

The origin of the unusual chemistry displayed by A-type magmas remains the subject of intense debate, many details of which are explored elsewhere in this

* Corresponding author. Fax: +61 0 8344 7761.
E-mail address: jhergt@unimelb.edu.au (J. Hergt).

0024-4937/$ - see front matter © 2006 Elsevier B.V. All rights reserved.
doi:10.1016/j.lithos.2006.12.008

volume. In brief, however, some have attributed distinctive chemical features to primary causes, such as the nature of mafic magmas from which A-types may have evolved (e.g., Loiselle and Wones, 1979; Turner et al., 1992; Qui et al., 2004) and/or the partial melting of unusual crustal source compositions (e.g., Collins et al., 1982; Clemens et al., 1986; Creaser et al., 1991; Frost and Frost, 1997; Wormald et al., 2004). Others propose that something extraordinary in the processes or conditions of magma formation and evolution can explain the resulting chemistry (e.g., unusually high temperature, low water contents or low pressures; e.g., King et al., 1997). The role of uncommonly low oxygen fugacity (fO_2) has also been proposed (e.g., Frost et al., 2001), although A-type magmas preserving primary magnetite have also been reported (e.g., Collins et al., 1982; Anderson and Bender, 1989; Qui et al., 2004; Dall'Agnol et al., 2005). Indeed, this highlights one of the outstanding problems in A-type studies in that a wide range of compositions has been described as "A-type" ranging from peraluminous through to metaluminous and peralkaline. Consequently, until such time as a consensus is reached regarding their classification, the various models proposed should therefore be examined in the context of the 'flavour' of A-type being described. Importantly, King et al. (1997, 2001) argued that because the compositions of the most evolved A-types of the Lachlan Fold Belt converge with high-silica I-type granites, the examination of suites of related granites spanning a wide range in silica contents is an essential prerequisite to the unambiguous identification and interpretation of A-type magmas.

To this end we have examined a suite of granitic rocks of Lachlan Fold Belt age from the Grampians region of western Victoria, Australia. Using new major, trace element and Sr, Nd and Hf isotope data, we explore the chemical features of this suite in the context of A-type and I-type classifications. We also use these geochemical data to examine the relationships between the weakly peraluminous–metaluminous and peralkaline members of the suite and identify the most likely source rocks from which these magmas were derived.

2. Regional setting

The Grampians Ranges of central western Victoria, Australia are located approximately 250 km west of Melbourne within a tectono-stratigraphic zone of complex history (Fig. 1). For many years the geological structure of the state of Victoria was divided into eight such zones on the basis of structural features and other criteria (e.g., chemical characteristics of granites), seven belonging to the Lachlan Fold Belt and the westernmost, the Glenelg Zone, representing the easternmost extent of the adjacent Adelaide Fold Belt (Vandenberg, 1978). The Grampians–Stavely Zone, located immediately east of the Glenelg Zone was, at that time, considered to represent the most westerly extent of the Lachlan Fold Belt. More recently, detailed mapping and additional geochronology (Cayley and Taylor, 1997; Stuart-Smith and Black, 1999) have revealed that the Grampians–Stavely Zone is better described as an area of complex transition from the Adelaide Fold Belt in the west and Lachlan Fold Belt to the east. Thus, in terms of its geological development, the Grampians region belongs to the Adelaide Fold Belt, and the steep east-dipping boundary between this, and the Lachlan Fold Belt has been placed at the Moyston Fault to the east of the Grampians Ranges (Fig. 1b). Nevertheless, extensive granitic magmatism of Lachlan Fold Belt age has taken place within the Grampians–Stavely Zone, one suite of which forms the focus of this study.

For the purpose of this paper, the more important aspects of the geological development of the Grampians–Stavely Zone can be summarised as follows (based on Cayley and Taylor, 1997). The basement rocks are believed to be Early (?) Cambrian submarine ultramafic to felsic volcanic rocks, possibly erupted in a back-arc basin environment, upon which sedimentary units (e.g., turbidites) were deposited, derived from cratonic sources located further west. During the early stages of the Delamerian Orogeny (~510 Ma) these rocks were deformed and the newly formed continental crust was accreted onto the Pacific margin of Gondwana. Further submarine eruptions, of felsic to intermediate composition, were subsequently covered by additional turbidite units and these were gently deformed. The end of the Delamerian Orogeny was marked by the emplacement of granites such as the Bushy Creek Granodiorite (495 Ma; Stuart-Smith and Black, 1999) located to the SE of the study area. Uplift and erosion of the Delamerian Highlands (to the west in the Adelaide Fold Belt) shed the substantial thicknesses of sediment which now constitutes the Grampians Group sedimentary rocks (more than 3.5 km thick, including fluviatile and shallow marine sequences). This sedimentary sequence was further thickened via thrust stacking during accretion of the Lachlan Fold Belt onto the Australian mainland in the Silurian, and subsequent large-scale folding. Approximately 15 km of shallow-angle extension along structures in the underlying basement in the Late(?) Silurian is sufficient to account for the observed extension in the Grampians Group, consistent with an asymmetric pull-apart system. This was followed by substantial erosion, generating areas

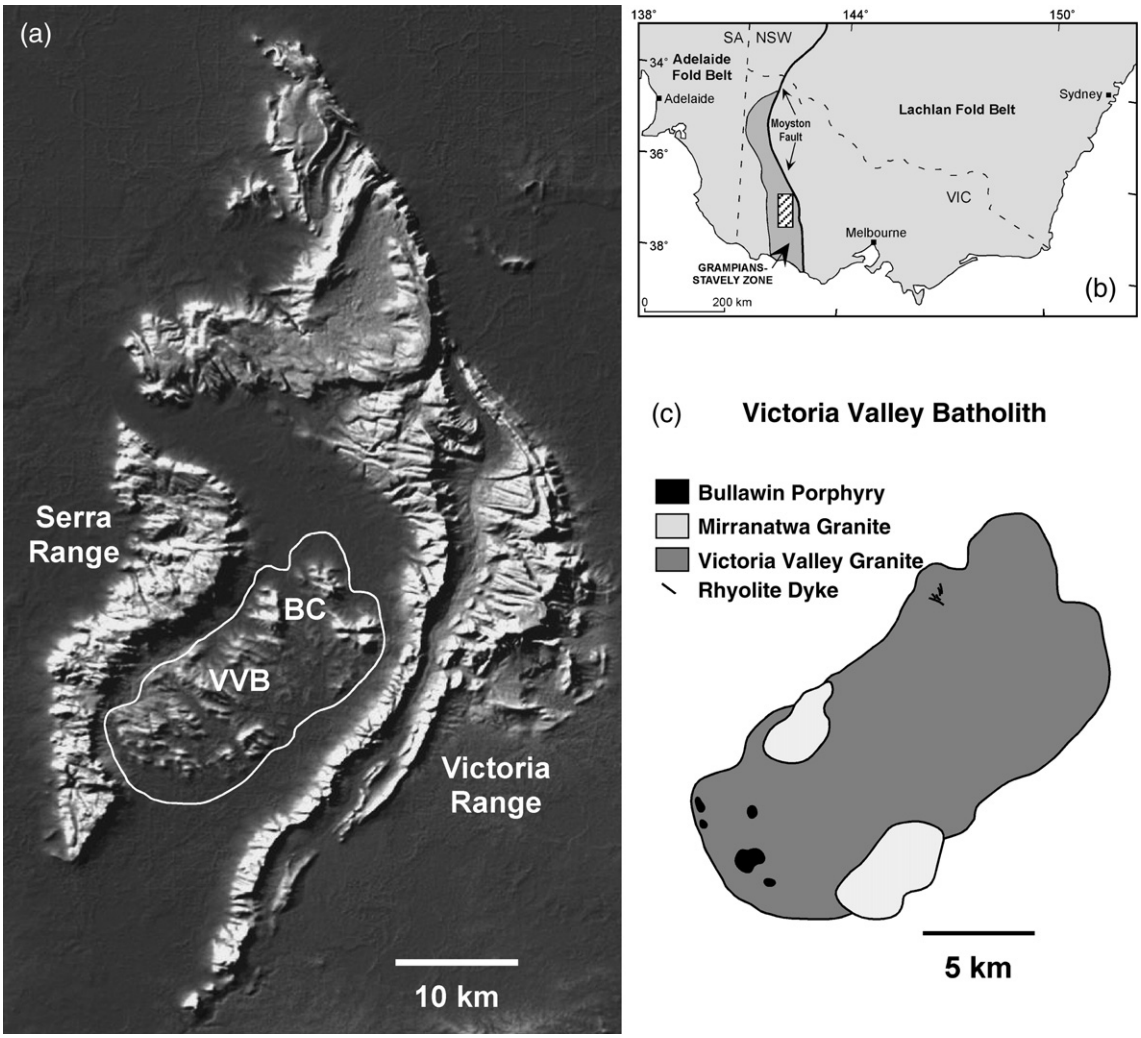

Fig. 1. Location and simplified geology of the Victoria Valley Batholith. a) Shuttle Radar Topography Mission (SRTM) image of the Grampians Ranges illustrating the location of the Victoria Valley Batholith (VVB) and the rhyolite dyke swarm on Big Chord ridge (BC) b) The location of the shaded relief map shown in a) is indicated by the shaded box relative to the Lachlan and Adelaide fold belts. The Lachlan Fold Belt is believed to terminate at the Moyston Fault. The Grampians–Stavely Zone is the easternmost extent of the Adelaide Fold Belt, but includes magmas of Lachlan Fold Belt age. State borders between Victoria, South Australia and New South Wales are shown using dashed lines c) Geological sketch map of the Victoria Valley Batholith illustrating the relationships between the main lithologies as defined by Cayley and Taylor (1997). SRTM image courtesy of M. Sandiford.

stripped back to bedrock prior to eruption of felsic volcanic rocks in the Early Devonian. This volcanism was accompanied by the shallow-level emplacement of granite plutons and dyke suites. Although dyke suites suggest syn-emplacement extension, variations in the orientations of these dykes suggest that localised stresses and pre-existing structures controlled the emplacement of these magmas.

It has been known for several decades that all of the granitic rocks within the Grampians–Stavely Zone are characterised by rather high bulk-rock Na_2O contents relative other I- and A-type granites. White and Chappell (1988) and Chappell et al. (1988) placed all of the granites into a single suite and argued that their high Na_2O and low K_2O "...suggests that this terrane is underlain by basaltic rocks in direct contrast to others of the Lachlan Fold Belt". On the basis of additional geochemistry, Chappell et al. (1991) placed the granites of the Victoria Valley Batholith into their own distinct suite. Importantly, granites of Delamerian age (e.g., the

495 Ma Bushy Creek pluton mentioned above) also occur within this same tectonic zone, and these preserve similarly high sodium contents as the Devonian granites suggesting a link between them, or their source rocks.

3. The Victoria Valley Batholith

The Victoria Valley Batholith, the focus of this paper, is ~390–395 Ma old (Richards and Singleton, 1981; Hergt, 1983, C. Gray pers. comm. in Cayley and Taylor, 1997) and is located between the two major strike ridges of the Grampians Group sediments, the Serra and Victoria Ranges (Fig. 1a).

3.1. Lithological units and petrography

Previously, numerous separate units have been described in the Victoria Valley Batholith (e.g., Atkinson, 1976; Hergt, 1983). In this study, we use the terms Victoria Valley Granite, Mirranatwa Granite and Bullawin Porphyry, following Cayley and Taylor (1997). A rhyolite dyke swarm described by Hergt (1983), along with smaller scattered rhyolite dykes, are referred to herein as a separate lithological unit (Fig. 1c).

3.1.1. Victoria Valley Granite

This unit is the most volumetrically abundant in the batholith (Fig. 1c). Where 'fresh', the Victoria Valley Granite is pale pink–grey and varies from fine- to medium-grained. Rocks are typically porphyritic, and generally preserve granophyric textures and miarolytic cavities consistent with a shallow level of emplacement; many rocks display pink to brick-red colouration, thought to represent hydrothermal alteration. The mineralogy is dominated by potassium-rich alkali–feldspar, quartz and plagioclase ($An_{18–30}$), with phenocryst cores generally ~$An_{25–30}$), along with minor biotite, calcic hornblende and accessory phases, the latter including opaque oxides, apatite, allanite, titanite and zircon.

3.1.2. Mirranatwa Granite

The Mirranatwa Granite is generally pinkish in colour and tends to be medium- to coarse-grained, typically even-grained but with some porphyritic variants. The mineralogy is dominated by perthitic alkali feldspar (up to 50%), quartz and plagioclase, with less than 10% mafic and accessory phases. The mafic mineralogy is the most distinctive feature of this granite. Although hornblende similar to that observed in the Victoria Valley Granite also occurs in these rocks, apple-green aegirine and sodium-rich amphiboles are typical of this unit. Variations in the pleochroic scheme of the sodic amphiboles, including brownish shades, suggest the occurrence of both riebeckite and arfvedsonite although MgO contents are invariably low (≤1%) and calculated atomic Fe^{2+}/Fe^{3+} averages ~2.5. The sodium-rich mafic minerals are usually ragged or skeletal, and are associated with quartz and opaques, apparently preserving a reaction relationship. Despite this, some euhedral diamond shapes are preserved, possibly indicating late-stage replacement of hornblende by both aegirine and sodic amphibole (sometimes accompanied by small grains of purple fluorite). Accessory phases include opaque oxides, zircon and apatite.

3.1.3. Bullawin Porphyry

We consider the naming of this most mafic phase to be unfortunate and unnecessarily ambiguous for this intrusive unit ('porphyry' being a name also associated with volcanic rocks). Nevertheless, this unit was probably the last to be emplaced in the main body of the complex, although the timing relationships between this unit and the rhyolite dykes are unknown. The rocks are fine- to medium-grained and are greyish-green where fresh. Even where fresh, the alkali feldspar is pink, and appears interstitial to plagioclase (~$An_{20–25}$) and quartz. Long needles of dark amphibole are clearly visible in hand specimen (up to 1 cm long) and euhedral plagioclase phenocrysts have cores of ~$An_{35–45}$. The amphibole is calcic, displays colourless to brown–green pleochroism, and the cores of grains are usually altered to yellow–brown biotite and pale-green chlorite. The composition is hornblende in which atomic Na+K varies from typical values (e.g., ~0.4 at $Al^{IV}=0.5$) to more elevated alkali contents closer to edenite (~0.8 at $Al^{IV}=1$). Accessory phases include opaque oxides, titanite, apatite and zircon.

Within the larger bodies of the Bullawin Porphyry are areas in which the typical lithology described above grades into more felsic variants. These tend to have biotite as the predominant mafic phase and the most felsic examples display a 'sugary' texture similar to aplites. To retain the context of these lithologies, one such example is presented in Table 1 as a 'felsic variant' with the Bullawin Porphyry entries.

3.1.4. Rhyolite dykes

The most extensive outcrop of rhyolite occurs in the northwestern part of the batholith, in vicinity of the Big Chord Ridge (Fig. 1a,c). Here the rhyolites comprise a network of dykes extending over approximately 1 km. The rocks are dark purple to red in colour and preserve delicate flow-banding that broadly parallels the dyke

margins. Close to the contact with the host granite, the flow-banding is highly contorted and spherulites are common. Although sharply-defined, the contact itself can be delicate, with small whisps of finely banded rhyolite injected into the granite host. The rhyolites are sufficiently glassy that even in thin-section it is difficult to discern more than the presence of quartz, possible feldspar and 'opaques'. Veins and dykes that are similar to these occur throughout the batholith, although most are too small to represent easily on geological maps.

Although outside the scope of this contribution, it is important to note the close relationship between the Victoria Valley Batholith, and other units in this region. In particular, widespread ($\sim$2000 km^2) felsic volcanic rocks occur west of the Victoria Range that closely match the Victoria and Mirranatwa granites in bulk-rock composition and petrographic features. Most of these volcanics are glassy and in thin-section reveal only quartz, feldspar (either K-feldspar or perthite) and opaques. In one location (Mt Cavendish) ragged peralkaline minerals associated with fluorite and rounded quartz phenocrysts were observed (Hergt, 1983) perhaps indicating that the expulsion of volatiles(?) from this felsic magma caused late-stage alteration of this volcanic pile similar to that observed in the Mirranatwa Granite. Broadly referred to as the Rocklands Rhyolite (Spencer-Jones, 1965), this unit comprises six large welded ignimbrites with a combined thickness of at least 250 m (Simpson, 1997). Other granitic bodies of the Grampians–Stavely Zone have been described (e.g., Spencer-Jones, 1965; Hergt, 1983). These include the Mafeking Granite located to the east of the Victoria Valley Batholith, and the MacKenzie River Granite located to the north. Both granites are similar in age to the Victoria Valley Batholith, and although these also display elevated Na_2O bulk-rock contents, they tend to lie away from the trends defined by the Victoria Valley Batholith rocks (Hergt, 1983).

4. Geochemistry of the Victoria Valley Suite: analytical methods and results

4.1. Samples and analytical approach

Here we present new major and trace element data for 35 samples of the Victoria Valley Batholith (Table 1). We have selected samples from the three lithologies of Cayley and Taylor (1997), making certain that these also represent units based on more detailed subdivisions (i.e., from Atkinson, 1976; Hergt, 1983). Only the most petrographically fresh materials have been analysed, obtained via collection involving the use of a rock drill where necessary and sledge hammers. All samples were crushed to gravel in a jaw-crusher, before being reduced to powder in an agate mill. The major element data were acquired using X-ray fluorescence spectrometry (XRF) and the work was conducted by Professor Bruce Chappell using well-established techniques widely reported in the literature (e.g., Hergt et al., 1989). In summary, the samples were fused in a lithium borate flux prior to major element analysis on a Spectro Analytical Instruments XLAB2000 polarising XRF spectrometer. Calibration was made against a wide range of international reference materials. Analytical precision is better than 0.5% relative and accuracy marginally greater than that. Trace element abundances were determined via inductively coupled plasma mass spectrometry (ICPMS) using the Varian quadrupole instrument in the School of Earth Sciences at the University of Melbourne. Around 100 mg of each sample was digested over 3 days in an HF–HNO_3 medium using Teflon pressure vessels in an oven set at 160 °C. These where then evaporated to dryness on a hotplate, refluxed in nitric acid, and dissolved in dilute HNO_3. An aliquot of each solution was spiked with a multi-isotope solution using procedures described in Eggins et al. (1997), except W-2 was employed as the calibration standard rather than BHVO-1. The latter was instead analysed as an unknown during the run and these data are provided as an illustration of precision and accuracy (Table 1).

From these samples, 19 were further analysed for their Rb–Sr and Sm–Nd isotopic compositions (Table 2). Whole-rock samples for isotope analysis were spiked with mixed ^{84}Sr–^{87}Rb and ^{149}Sm–^{150}Nd tracers, and dissolved in Teflon bombs over a period of several days using a combination of HF, HNO_3, and HCl acids. Rb, Sr, Sm, and Nd were separated by conventional ion exchange methods, with analytical blanks being negligible in all cases. Separated samples were run on an Nu Plasma MC-IC PMS with sample introduction by an Aridus desolvation

Notes to Table 1:
Trace element data for VV13 are based on the XRF analysis of pressed powder pellets. The nomenclature for rock units employed in earlier studies is provided to aid comparisons, but the unit names of Cayley and Taylor (1997) are used herein. The Aluminium Saturation Index (ASI) is the value of molecular $Al_2O_3/(Na_2O+K_2O+(CaO-3.3xP_2O_5)$. The Al/Na+K is the value for molecular Al_2O_3/Na_2O+K_2O. Temp. °C refers to the zircon saturation temperature calculated according to Watson and Harrison (1983). The average trace element determination of BHVO-1 based on 5 independent dissolutions and analysis over the analytical session (4 different days) is provided, together with reported values (from Eggins et al., 1997, but with the values for Y, Zr and Nb adjusted to lower values according to the work of Makishima et al., 1999; Reid et al., 1999; Robinson et al., 1999).

unit, modified to use a Glass Expansion 'OpalMist' nebuliser, operating at an uptake rate of ~30 μlmin^{-1}. All analyses were performed in static multicollection mode. In the following 'SD' refers to standard deviation on the mean, whereas 'se' refers to the standard error on individual determinations.

Table 1
Bulk-rock major (wt.% oxide) and trace element (ppm) data for 35 samples of the Victoria Valley Batholith (see text for analytical protocols)

Name	Bullawin Porphyry								Mirranatwa Granite					
Previous subdivision	Bare Hill Rhyodacite							Felsic variant	Knights Hill Aegirine Granite				Western Aegirine Granite	
GRID REF	112587	111588	148550	136562	141552	148549	144574	134567	213566	223566	222566	221568	162630	151631
Sample No.	VV1	VV2	VV3	VV4	VV5	VV6	VV7	VV8	VV9	VV10	VV11	VV12	VV13	VV14
SiO2	65.26	66.95	66.96	67.28	68.46	69.95	70.04	77.76	72.35	73.17	77.34	78.25	77.99	78.34
TiO2	0.70	0.70	0.92	0.76	0.57	0.57	0.46	0.13	0.34	0.30	0.16	0.11	0.13	0.13
Al2O3	15.62	15.62	15.74	15.89	15.40	14.95	15.39	12.41	14.02	13.64	11.21	11.37	11.68	11.34
FeO(Total)	6.40	4.44	3.72	3.56	3.65	3.09	2.74	0.68	2.37	2.73	2.42	2.16	1.59	1.65
MnO	0.11	0.12	0.09	0.14	0.04	0.07	0.08	0.00	0.05	0.04	0.02	0.00	0.01	0.03
MgO	0.95	0.97	1.37	1.22	0.82	0.71	0.66	0.02	0.31	0.23	0.06	0.03	0.05	0.03
CaO	2.57	2.59	3.10	2.89	2.31	2.04	1.77	0.25	0.94	0.75	0.05	0.02	0.04	0.08
Na2O	5.59	5.62	4.93	4.75	5.46	4.99	5.15	3.82	5.35	4.86	4.43	3.79	3.93	3.96
K2O	2.62	2.78	2.93	3.28	3.14	3.52	3.61	4.92	4.22	4.24	4.29	4.26	4.57	4.44
P2O5	0.19	0.20	0.24	0.22	0.16	0.12	0.10	0.01	0.05	0.04	0.01	0.01	0.01	0.01
Li	11.4	11.9	24.7	24.7	38.5	28.1	35.4	10.3	13.3	23.3	61.7	2.1		16.6
Be	2.4	3.2	2.6	2.6	2.7	3.0	2.8	3.4	3.3	2.7	6.2	2.6		3.6
Sc	11.7	10.6	10.7	8.7	8.3	7.8	5.4	3.0	6.5	5.9	1.1	0.9		0.9
V	9.8	14.3	46.6	45.4	21.4	21.7	21.2	2.0	5.7	4.6	1.5	0.4		0.6
Cr	1.0	0.3	0.9	0.3	2.1	0.3	3.1	6.5	0.9	4.7	1.8	0.3		0.5
Co	34.2	35.7	5.6	5.3	4.8	3.6	4.4	0.3	37.4	45.9	54.7	55.0		60.4
Ni	1.5	1.3	0.2	0.6	0.6	0.5	1.6	0.6	0.9	1.0	0.6	0.6		0.6
Cu	6.5	8.4	3.2	2.7	4.3	8.2	5.0	1.9	5.7	6.4	5.0	2.3	2	4.1
Zn	92	88	53	53	70	72	63	16	36	38	167	31	38	78
Ga	20.1	19.8	17.5	18.3	16.6	17.0	17.8	15.6	18.2	18.3	23.0	21.5	23.2	23.7
As	3.90	3.40	1.56	0.81	1.42	0.80	0.38	0.91	2.50	0.75	2.15		0.70	0.90
Rb	82	93	115	99	119	151	129	230	144	137	196	132	185	172
Sr	200	192	312	419	179	216	162	17	57	46	5	4	15	8
Y	45.0	68.2	31.8	26.8	37.3	32.6	28.6	35.0	40.2	45.6	83.8	46.8	99.5	159.3
Zr	401	406	313	265	406	355	468	160	393	402	870	493	522	802
Nb	16.4	14.5	17.2	16.2	13.2	16.0	13.3	15.7	16.3	13.7	33.3	17.8	28.2	25.8
Mo	3	4	1	2	2	3	5	4	3	4	2	1	1.3	3
Cd	0.170	0.181	0.120	0.079	0.093	0.192	0.137	0.033	0.115	0.098	0.165	0.071		0.188
Sn	3.2	2.7	2.0	1.9	3.7	4.8	1.0	3.5	4.5	3.9	8.8	4.7	7.4	6.0
Sb	0.34	0.90	0.24	0.14	0.27	0.16	0.07	0.19	0.68	0.34	0.94	0.43		0.24
Cs	3.0	5.1	6.7	4.8	6.0	5.4	6.5	7.0	3.9	5.3	3.3	1.4	1	2.9
Ba	528	451	594	804	484	603	733	270	640	570	85	96	128	105
La	41.0	53.9	43.7	54.3	33.1	45.7	39.2	36.9	42.1	58.0	85.0	16.3	84.8	320.8
Ce	81	102	86	101	71	89	75	88	83	107	161	36	178	515
Pr	10.08	12.85	9.96	11.22	8.11	10.07	7.77	7.84	9.85	12.54	19.16	4.12		75.48
Nd	38.8	50.7	36.5	38.2	30.4	35.2	26.7	25.9	35.8	44.2	67.6	15.2	75	279.0
Sm	8.11	10.71	6.81	6.66	6.24	6.53	4.86	5.13	7.24	8.41	13.61	3.63		58.07
Eu	2.03	2.50	1.61	1.60	1.30	1.37	1.08	0.24	1.06	1.03	0.98	0.35		4.28
Gd	8.10	11.96	6.21	5.65	6.17	5.94	4.56	4.93	6.80	7.90	12.99	4.82		48.53
Tb	1.29	1.88	0.97	0.84	1.03	0.96	0.75	0.90	1.14	1.31	2.26	1.10		6.59
Dy	7.87	11.35	5.75	4.87	6.43	5.84	4.68	5.72	7.05	7.97	14.11	7.81		33.03
Ho	1.68	2.46	1.21	1.00	1.36	1.22	1.00	1.25	1.52	1.71	3.10	1.79		5.84
Er	4.73	6.79	3.40	2.77	3.97	3.53	3.01	3.72	4.43	4.90	9.14	5.36		14.19
Tm	0.710	0.979	0.511	0.414	0.607	0.541	0.471	0.598	0.686	0.746	1.423	0.840		1.928
Yb	4.50	6.03	3.31	2.60	3.93	3.51	3.17	3.97	4.49	4.81	9.29	5.49		11.32
Lu	0.679	0.893	0.487	0.382	0.596	0.525	0.492	0.589	0.677	0.719	1.378	0.813		1.595
Hf	8.9	9.1	7.2	6.4	9.1	8.5	10.0	5.5	9.6	9.7	20.5	11.4	17.1	17.7
Ta	1.1	1.1	1.2	1.1	1.0	1.2	1.0	1.5	1.3	1.3	2.3	1.5	3.6	2.0
Tl	0.497	0.462	0.874	0.559	0.856	0.761	0.778	0.516	0.640	0.656	0.879	0.818	1.6	0.813
Pb	19.5	18.9	20.2	12.5	19.7	25.5	21.0	20.5	19.6	19.1	25.7	6.6	17.2	27.7
Th	9.87	12.18	14.01	15.10	15.72	17.42	17.75	30.47	17.46	17.16	27.67	15.99	30	22.20
U	2.55	2.98	3.26	3.14	4.03	4.07	4.41	6.03	4.23	4.08	6.12	3.20	6	6.34
ASI	0.96	0.95	0.96	0.99	0.95	0.97	1.00	1.03	0.94	0.98	0.93	1.05	1.02	0.99
A/Na+K	1.30	1.27	1.40	1.40	1.24	1.24	1.24	1.07	1.05	1.08	0.94	1.05	1.02	1.00
Temp. °C	845	847	825	813	852	846	878	794						

Table 1 (*continued*)

Name	Victoria Valley Granite										
Previous subdivision	Ferrohastingsite Dellenite	Green Hill Adamellite	Longreach Adamellite						Mirranatwa Granophyre		
GRID REF	227581	215699	281643	271586	301668	304654	168547	143571	243692	137592	167587
Sample No.	VV15	VV16	VV17	VV18	VV19	VV20	VV21	VV22	VV23	VV24	VV25
SiO2	72.92	75.14	73.88	73.63	74.45	74.61	74.84	76.25	74.62	74.80	74.89
TiO2	0.29	0.25	0.29	0.29	0.31	0.28	0.25	0.19	0.26	0.23	0.25
Al2O3	13.67	13.07	13.27	13.93	13.66	13.49	13.34	12.98	13.18	13.47	13.30
FeO(Total)	2.46	1.91	2.76	1.86	1.78	1.68	1.65	1.11	2.14	1.59	1.45
MnO	0.06	0.02	0.04	0.06	0.05	0.04	0.06	0.01	0.03	0.05	0.02
MgO	0.33	0.22	0.47	0.35	0.39	0.33	0.27	0.16	0.25	0.23	0.28
CaO	1.38	0.84	1.11	1.16	1.33	1.08	0.72	0.52	0.77	0.75	0.69
Na2O	5.04	4.17	4.10	4.32	4.10	4.22	4.37	3.96	4.17	4.42	4.53
K2O	3.80	4.35	4.02	4.35	3.88	4.21	4.44	4.82	4.52	4.43	4.56
P2O5	0.05	0.03	0.06	0.05	0.06	0.05	0.04	0.01	0.04	0.04	0.03
Li	10.5	28.9	38.0	53.7	17.7	30.6	21.3	15.9	51.1	14.9	14.0
Be	2.8	3.4	2.9	3.1	2.8	2.8	3.2	2.8	3.0	2.7	3.1
Sc	6.6	3.6	4.4	4.2	4.3	3.7	3.6	3.2	3.6	4.1	3.8
V	9.9	6.1	13.2	10.7	14.1	11.9	8.4	4.7	8.6	8.1	7.8
Cr	2.3	8.4	2.0	1.6	1.9	1.0	1.1	0.6	11.3	3.0	2.6
Co	44.7	59.3	38.9	45.0	41.9	57.1	47.2	1.2	48.1	1.9	38.5
Ni	1.3	13.9	2.2	1.6	1.9	1.5	1.4	0.9	1.7	1.1	1.4
Cu	8.4	10.5	4.1	7.5	3.9	9.1	7.7	3.8	6.5	3.4	26.1
Zn	134	22	32	76	42	50	46	83	45	45	40
Ga	16.7	15.0	15.2	16.1	15.4	15.6	16.0	15.5	15.7	16.1	16.1
As	2.00	1.05	1.50	1.20	0.40	2.10	0.50	0.72	1.15	0.99	0.50
Rb	152	173	151	178	148	172	182	198	185	175	169
Sr	99	67	108	92	88	94	76	42	66	73	69
Y	33.0	28.1	27.5	27.0	25.2	24.5	28.1	27.9	27.7	31.4	29.0
Zr	274	202	249	244	222	194	237	205	236	251	251
Nb	8.9	10.0	9.7	7.5	10.5	10.6	11.6	13.3	11.8	13.1	12.6
Mo	2	4	3	5	2	2	5	3	7	3	1
Cd	0.110	0.060	0.064	0.164	0.077	0.150	0.147	0.035	0.131	0.051	0.110
Sn	5.1	3.7	3.8	4.0	2.6	2.8	3.0	4.1	3.6	3.8	5.3
Sb	0.76	0.32	0.31	0.31	0.52	0.59	0.14	0.08	0.21	0.17	0.24
Cs	4.4	6.4	5.9	11.0	3.7	4.7	7.0	4.5	6.0	4.8	4.3
Ba	550	457	600	659	598	536	597	582	590	612	603
La	30.2	39.4	36.3	36.7	36.0	39.3	37.7	44.7	40.2	44.3	40.3
Ce	62	69	65	69	67	67	69	80	74	81	74
Pr	7.43	7.55	7.10	7.37	7.14	7.38	7.43	8.47	7.84	8.64	8.05
Nd	27.8	25.0	24.1	24.7	23.8	24.2	24.6	27.6	25.6	28.5	26.7
Sm	5.90	4.60	4.44	4.66	4.38	4.37	4.64	5.02	4.65	5.23	5.01
Eu	1.11	0.58	0.76	0.75	0.77	0.73	0.59	0.50	0.60	0.62	0.61
Gd	5.67	4.19	4.09	4.29	4.01	3.97	4.33	4.57	4.23	4.87	4.60
Tb	0.95	0.73	0.69	0.72	0.67	0.65	0.74	0.76	0.71	0.82	0.78
Dy	5.78	4.53	4.27	4.49	4.13	3.97	4.62	4.77	4.53	5.15	4.83
Ho	1.24	1.00	0.95	0.97	0.89	0.86	1.00	1.02	0.99	1.11	1.05
Er	3.57	2.98	2.82	2.86	2.62	2.51	2.97	2.99	2.93	3.26	3.11
Tm	0.550	0.482	0.449	0.455	0.417	0.399	0.470	0.477	0.467	0.514	0.497
Yb	3.58	3.24	2.95	3.05	2.81	2.66	3.16	3.16	3.12	3.45	3.31
Lu	0.536	0.489	0.454	0.462	0.428	0.406	0.482	0.478	0.480	0.519	0.503
Hf	7.0	5.7	6.4	6.2	5.7	5.2	6.3	5.9	6.2	6.8	6.7
Ta	1.0	1.5	1.2	0.9	1.0	1.1	1.1	1.2	1.0	1.2	1.1
Tl	0.885	0.789	0.984	0.997	0.711	0.692	0.782	0.946	0.869	0.837	1.331
Pb	28.2	19.8	21.4	23.4	24.6	23.7	24.2	25.0	19.0	21.9	15.2
Th	14.44	25.51	20.61	22.45	20.59	21.15	23.60	25.36	24.34	22.97	22.35
U	3.16	5.37	4.15	5.24	3.79	5.33	5.27	5.10	5.99	5.43	5.45
ASI	0.92	1.00	1.02	1.01	1.03	1.01	1.01	1.03	1.01	1.01	0.98
A/Na+K	1.10	1.13	1.20	1.18	1.25	1.17	1.11	1.11	1.12	1.12	1.07
Temp. °C	822	808	827	823	819	804	823	814	822	828	825

$^{87}Sr/^{86}Sr$ data are normalised to a 'recommended' value for NIST SRM 987 of 0.710230, with actual data obtained during the analytical session of 0.710120±9 (2sd, $n=4$). A secondary standard, BCR-2, gave a normalised value of 0.704954, while the GLO-1 glauconite standard produced an age of 83.7 Ma, assuming an initial $^{87}Sr/^{86}Sr$ ratio of

Name	Victoria Valley Granite									Rhyolite	BHVO-1	
Previous subdivision	Mirranatwa Granophyre							Strachans Hut Adamellite		Rhyolite	Average $n=5$ (this study)	Reported Values
GRID REF	169585	201595	230611	146586	245655	212631	194635	138628	139629	111588		
Sample No.	VV26	VV27	VV28	VV29	VV30	VV31	VV32	VV33	VV34	VV35		
SiO2	75.09	75.50	75.70	76.03	76.77	76.83	78.34	73.84	73.38	75.56		
TiO2	0.26	0.23	0.25	0.22	0.21	0.18	0.13	0.30	0.31	0.22		
Al2O3	13.25	13.08	13.29	12.83	13.01	12.93	12.24	14.05	13.80	13.11		
FeO(Total)	1.54	1.38	1.33	1.30	1.04	0.87	0.49	2.04	2.32	1.54		
MnO	0.02	0.03	0.03	0.03	0.00	0.00	0.01	0.02	0.08	0.02		
MgO	0.31	0.22	0.18	0.18	0.07	0.15	0.08	0.14	0.23	0.12		
CaO	0.60	0.60	0.22	0.59	0.18	0.60	0.33	0.47	0.70	0.53		
Na2O	4.39	4.23	4.24	3.98	3.87	3.76	3.85	4.86	4.96	4.61		
K2O	4.50	4.70	4.73	4.83	4.84	4.64	4.52	4.23	4.17	4.25		
P2O5	0.04	0.03	0.04	0.02	0.02	0.02	0.01	0.04	0.05	0.03		
Li	19.9	8.4	9.3	10.0	9.8	22.7	8.2	7.2	9.5	4.7	4.6	4.90
Be	3.2	3.0	3.5	3.5	3.2	3.4	2.9	2.8	3.8	2.7	0.9	1.10
Sc	3.8	3.0	3.4	3.7	3.0	2.8	3.9	6.0	6.1	5.1	30.7	31.8
V	7.7	6.0	6.7	5.3	4.6	4.8	0.9	4.7	4.9	1.5	293	321
Cr	1.1	0.9	1.1	0.8	0.9	1.0	0.3	1.9	2.6	0.3	283	289
Co	41.7	38.9	43.9	43.3	46.2	53.3	61.8	38.2	40.3	48.5	44	45
Ni	1.3	1.2	0.8	1.1	0.8	0.6	0.2	0.5	0.7	0.2	112	120
Cu	31.3	3.5	3.7	5.0	2.6	2.9	29.6	3.3	4.1	4.6	129	136
Zn	26	30	26	31	34	15	33	24	42	19	105	105
Ga	15.9	13.9	15.5	15.5	14.5	14.7	13.1	18.4	18.3	16.4	20.7	21
As	0.40	1.40	0.70	0.80	1.10	0.50	0.30	1.25	1.30	1.90	0.5	
Rb	180	158	173	185	197	213	181	142	145	140	9.2	9.5
Sr	63	42	44	54	42	50	31	52	54	42	387	390
Y	29.9	23.4	25.7	30.5	25.5	38.0	42.2	38.2	45.7	39.6	24.0	*24.6*
Zr	267	211	235	221	177	180	120	439	479	325	171	*170*
Nb	12.4	10.3	10.2	13.9	12.4	8.1	7.0	14.1	15.0	8.3	18.6	*18.8*
Mo	2	2	2	5	2	2	3	3	4	1	1	1.0
Cd	0.093	0.056	0.061	0.084	0.039	0.046	0.376	0.088	0.126	0.084	0.104	0.069
Sn	9.1	5.6	3.1	4.2	3.8	2.5	4.6	4.9	4.5	1.7	1.9	2.30
Sb	0.27	0.33	0.38	0.19	0.27	0.12	0.17	0.37	0.33	0.38	0.14	0.170
Cs	6.1	2.2	2.5	3.8	4.8	5.4	3.6	4.1	3.2	3.4	0.1	0.100
Ba	587	677	595	565	547	467	563	601	577	538	133	133
La	39.5	38.3	42.4	40.6	47.3	65.4	57.6	53.9	41.8	40.0	15.2	15.5
Ce	74	69	77	75	91	115	109	141	85	75	37	38.0
Pr	8.03	7.29	8.15	7.97	9.41	12.30	12.43	16.45	9.90	9.02	5.44	5.45
Nd	26.9	23.6	26.3	26.4	29.7	39.7	42.9	53.3	35.5	32.0	24.7	24.7
Sm	5.04	4.24	4.70	5.02	5.20	7.37	8.20	10.53	7.33	6.47	6.10	6.17
Eu	0.56	0.48	0.53	0.47	0.60	0.73	0.76	1.47	0.99	0.68	2.05	2.06
Gd	4.67	3.73	4.18	4.61	4.32	6.74	7.29	7.11	7.12	6.26	6.17	6.22
Tb	0.79	0.63	0.70	0.79	0.72	1.14	1.18	1.22	1.21	1.07	0.94	0.95
Dy	5.01	3.94	4.34	5.01	4.36	6.99	7.20	7.14	7.64	6.80	5.21	5.25
Ho	1.08	0.85	0.94	1.09	0.93	1.44	1.51	1.43	1.67	1.46	1.00	1.00
Er	3.19	2.52	2.79	3.27	2.75	4.15	4.32	4.19	4.89	4.27	2.49	2.56
Tm	0.508	0.408	0.448	0.524	0.444	0.659	0.665	0.677	0.764	0.678	0.334	
Yb	3.41	2.73	3.04	3.53	2.98	4.35	4.25	4.54	4.99	4.41	1.98	1.98
Lu	0.516	0.420	0.465	0.533	0.454	0.638	0.626	0.693	0.755	0.660	0.272	0.278
Hf	7.0	5.7	6.3	6.3	5.1	5.3	3.9	10.4	11.2	8.5	4.3	4.30
Ta	1.1	1.0	1.0	1.2	1.1	1.7	1.1	1.3	1.4	1.3	1.2	1.200
Tl	1.440	0.783	0.861	0.933	0.827	0.772	0.859	0.656	0.668	0.493	0.039	0.059
Pb	15.1	17.2	18.8	18.9	17.8	19.7	20.3	17.1	13.9	15.8	2.1	2.10
Th	23.51	23.35	25.85	25.50	24.87	31.34	22.58	17.59	18.39	18.68	1.19	1.26
U	5.43	5.11	5.71	5.29	6.10	8.44	6.97	4.79	4.80	4.79	0.44	0.420
ASI	1.01	1.00	1.07	1.00	1.09	1.06	1.04	1.05	1.00	1.00		
A/Na+K	1.10	1.09	1.10	1.09	1.12	1.15	1.09	1.12	1.09	1.08		
Temp. °C	835	812	830	818	808	806	771	887	887	853		

0.71 (known age ~84 Ma). Within-run errors are typically ≤±0.000020 (2se). $^{143}Nd/^{144}Nd$ data are normalised to a 'recommended' value for La Jolla Nd of 0.511860, with actual data obtained during the analytical session of 0.511830±9 (2sd, $n=6$). Within-run errors are typically ≤±0.000010 (2se).

Table 2
Rb–Sr and Sm–Nd data for 19 of the samples of this study

Lithology	Sample	Rb ppm	Sr ppm	87Rb/86Sr	87Sr/86Sr	Sm ppm	Nd ppm	147Sm/144Nd	143Nd/144Nd	87Sr/86Sri	143Nd/144Ndi
Bullawin Porphyry	VV1	82.09	203.86	1.165	0.711041	8.06	38.65	0.1261	0.512560	0.704470	0.512233
	VV2	92.94	194.23	1.385	0.712239	10.84	51.41	0.1275	0.512521	0.704430	0.512190
	VV9	146.58	58.26	7.305	0.745696	7.47	37.36	0.1209	0.512531	0.704500	0.512217
	VV10	134.98	46.32	8.465	0.751345	8.41	44.95	0.1131	0.512526	0.703608	0.512233
Mirranatwa Granite	VV11	201.32	4.37	142.121	1.379331	12.11	59.91	0.1222	0.512552	0.577906	0.512236
	VV12	131.50	3.85	104.134	1.258158	3.37	14.65	0.1389	0.512585	0.670942	0.512225
	VV13	176.24	8.40	62.763	1.058522	59.27	300.32	0.1193	0.512537	0.704600	0.512228
	VV15	153.65	99.81	4.463	0.730987	5.93	28.21	0.1270	0.512418	0.705819	0.512088
	VV16	180.37	67.66	7.742	0.748093	4.98	26.95	0.1116	0.512476	0.704433	0.512186
	VV18	175.24	87.58	5.804	0.736391	4.46	24.12	0.1119	0.512477	0.703660	0.512187
	VV19	146.23	86.41	4.907	0.732831	4.48	24.50	0.1107	0.512451	0.705158	0.512164
Victoria Valley Granite	VV23	186.60	65.22	8.312	0.751243	4.76	26.66	0.1080	0.512487	0.704373	0.512207
	VV25	166.67	68.84	7.030	0.744594	4.98	27.08	0.1112	0.512495	0.704954	0.512207
	VV27	187.39	50.08	10.885	0.766347	5.03	27.87	0.1091	0.512485	0.704965	0.512203
	VV30	207.83	44.81	13.512	0.781274	5.54	32.06	0.1046	0.512466	0.705081	0.512195
	VV32	182.57	31.91	16.700	0.798758	8.38	44.32	0.1143	0.512436	0.704588	0.512140
	VV33	143.60	53.07	7.860	0.748779	10.70	55.18	0.1172	0.512506	0.704458	0.512202
	VV34	146.64	53.22	8.004	0.749898	7.51	37.04	0.1225	0.512544	0.704764	0.512226
Rhyolite	VV35	141.35	42.27	9.720	0.758185	6.56	32.66	0.1214	0.512520	0.703375	0.512205

Refer to Section 4.1 for details of the analytical techniques employed. The initial isotope ratios calculated for an age of 396 Ma are given by $^{87}Sr/^{86}Sri$ and $^{143}Nd/^{144}Nd_i$.

Finally, the Hf isotope compositions (Table 3) were determined for zircons separated from three samples (representing the three units of Cayley and Taylor, 1997). Zircons for Hf-isotope analysis were mounted in epoxy blocks and polished to reveal internal surfaces. Hf-isotope measurements were performed with an excimer laser ablation microprobe, coupled to the Nu Plasma MC -ICPMS as described in some detail in Woodhead et al. (2004). A laser spot size of ~50 μm was used with repetition rate of 5 Hz and power density <5 J cm^{-2}. This was sufficient to achieve total Hf signals of 5–10 V. Analysis of the 91500, Temora, and BR-266 zircons during the course of this study provided $^{176}Hf/^{177}Hf$ values of 0.282303±13 (2sd, n=3), 0.282691±16 (2sd, n=6) and 0.281629±8 (2sd, n=2) which compare well with the solution-ICPMS 'bulk' analysis values recommended by Woodhead and Hergt (2005) of 0.282306, 0.282686, and 0.281630 respectively.

4.2. Major and trace element variations: are these rocks A-types?

Whole-rock analyses for samples from the Victoria Valley Batholith range in SiO_2 from ~65–78 wt.%. Strong correlations are generally observed between most major and trace elements with increasing silica, and Fig. 2a illustrates the high Na_2O in these rocks, compared with typical Lachlan Fold Belt I-types as well as the less common A-types. As expected, the sodium contents in the Victoria Valley rocks are elevated, particularly in the more mafic member of the suite (the Bullawin Porphyry) and persist to higher silica, although values converge at around 78 wt.%. At around 65 wt.% SiO_2 however, the Bullawin Porphyry samples have ~5.5% Na_2O, approximately twice that of Lachlan Fold Belt I-types at the same silica content. Furthermore, unlike other Lachlan Fold Belt granites in which Na_2O shows little variation with increasing SiO_2, the Victoria Valley rocks preserve a marked negative correlation.

In contrast, the K_2O contents for this suite are similar to Lachlan Fold Belt I-type granites, and perhaps slightly lower than Lachlan Fold Belt A-types at similar silica (Fig. 2b). In all cases, the K_2O contents increase with increasing SiO_2, but the K_2O contents never reach the very high levels described for some A-types such as the Pikes Peak, Wolf River and Sherman batholiths of the USA (e.g., Frost and Frost, 1997). Finally, the abundances of Al_2O_3 tend to be slightly higher in the Victoria Valley suite than both I- and A-types of the Lachlan Fold Belt (Fig. 2c), with CaO contents relatively low and most similar to A-types (Fig. 2d). On balance, the rocks of the Victoria Valley suite are metaluminous to weakly peraluminous (ASI=0.9–1.1), with only VV11 having molecular $Al_2O_3/(Na_2O+K_2O)$ <1 (Table 1), despite the high sodium contents across the entire suite, and the appearance of peralkaline minerals in the Mirranatwa Granite.

Table 3
Laser ablation Lu–Hf isotope data measured in zircons separated from three of the samples of this study

Sample	Analysis No.	176Hf/177Hf	uncertainty (2σ)	176Lu (ppm)	176Yb (ppm)	176Lu/177Hf	176Hf/177Hfi
Bullawin Porphyry (VV1)	1	0.282888	0.000040	11,914	528,004	0.007299	0.282834
	2	0.282845	0.000036	11,130	476,987	0.006173	0.282799
	3	0.282845	0.000036	12,238	525,555	0.007518	0.282789
	4	0.282837	0.000046	12,071	518,246	0.007179	0.282784
	5	0.282922	0.000048	13,239	571,606	0.008990	0.282855
	6	0.282927	0.000042	12,196	533,402	0.007532	0.282871
	7	0.282779	0.000042	8,942	368,532	0.004028	0.282749
	8	0.282956	0.000084	8,253	340,103	0.004397	0.282923
	9	0.282821	0.000062	7,695	311,278	0.003552	0.282795
	10	0.282906	0.000048	10,788	471,493	0.006162	0.282860
	11	0.282924	0.000038	10,267	430,123	0.005222	0.282885
	12	0.283041	0.000076	11,209	501,390	0.006563	0.282992
	13	0.282961	0.000030	12,422	568,725	0.008312	0.282899
	14	0.282834	0.000058	7,661	319,820	0.003238	0.282810
	15	0.283003	0.000042	12,383	553,316	0.008018	0.282943
	16	0.282896	0.000046	10,822	480,595	0.005988	0.282851
	17	0.282766	0.000064	8,106	309,307	0.003337	0.282741
	18	0.283015	0.000054	9,546	395,548	0.004568	0.282981
	19	0.283057	0.000086	8,971	369,150	0.004347	0.283025
Mirranatwa Granite (VV11)	1	0.282988	0.000098	11,028	583,559	0.008045	0.282928
	2	0.283080	0.000058	12,692	597,489	0.009200	0.283012
	3	0.283091	0.000092	12,894	683,602	0.011717	0.283004
	4	0.283038	0.000056	11,180	582,819	0.007784	0.282980
	5	0.282975	0.000056	12,481	621,533	0.009659	0.282903
Victoria Valley Granite (VV33)	1	0.283111	0.000260	13,518	472,623	0.007450	0.283056
	2	0.282832	0.000052	11,923	451,377	0.006172	0.282786
	3	0.283135	0.000056	13,114	557,538	0.008601	0.283071

Corrections for the unusually large isobaric interferences on mass 176 degrade the reproducibility of the final $^{176}Hf/^{177}Hf$ ratios by a factor of around 3 relative to more typical zircons analysed under the same run conditions. Age corrected data provide initial ratios ($^{176}Hf/^{177}Hf_i$) at 396 Ma.

King et al. (1997) provide a useful summary of the features typical of A-type granites in the Lachlan Fold Belt. These include a shallow level of emplacement, high $Fe_{(total)}/Fe_{(total)}+MgO$, and low CaO and Sr compared with I-type granites. Clearly, based on the descriptions provided above, the Victoria Valley Batholith displays several of these features. These include the shallow level of their emplacement indicated by the presence of miarolytic cavities, graphic intergrowth, porphyritic textures and association with rhyolite dykes and felsic volcanic rocks of similar composition. In addition, the low CaO contents are well illustrated in Fig. 2d and Sr preserves a similar relationship with Lachlan Fold Belt A-types (not shown).

In addition to the broad features shared by Lachlan Fold Belt A-type granites, several authors have proposed discrimination diagrams specifically for the purpose of classification. In the two examples shown here, the Victoria Valley rocks extend into the A-type field (Fig. 3). King et al. (1997, 2001) suggest that a distinctive feature of the Lachlan Fold Belt A-types is their high Zr content (Fig. 4a), particularly in granites with lowest silica, accompanied by high zircon saturation temperatures (calculated according to Watson and Harrison, 1983). The high Zr abundances of the Victoria Valley rocks show clearer affinities with Lachlan Fold Belt A-type samples than I-types. Importantly, this feature persists in the samples of the Bullawin Porphyry at the lowest silica contents. At the highest silica contents (~78 wt.%) four samples of the Mirranatwa Granite plot away from the main data array at extraordinarily high Zr contents (VV11–VV14). This is unusual compared with both A- and I-type granites from the Lachlan Fold Belt, but typical of peralkaline granites and "problematic I-types" believed to have experienced substantial alteration (King et al., 1997).

As in the A-type studies of previous authors, zircon saturation temperatures have been calculated for the samples in this study (Table 1). Zircons for the Victoria Valley Granite and Bullawin Porphyry lack inheritance, display magmatic zonation and preserve euhedral morphologies. In contrast, values for the Mirranatwa Granite have not been included as these grains are highly irregular in shape and are likely to be hydrothermal rather

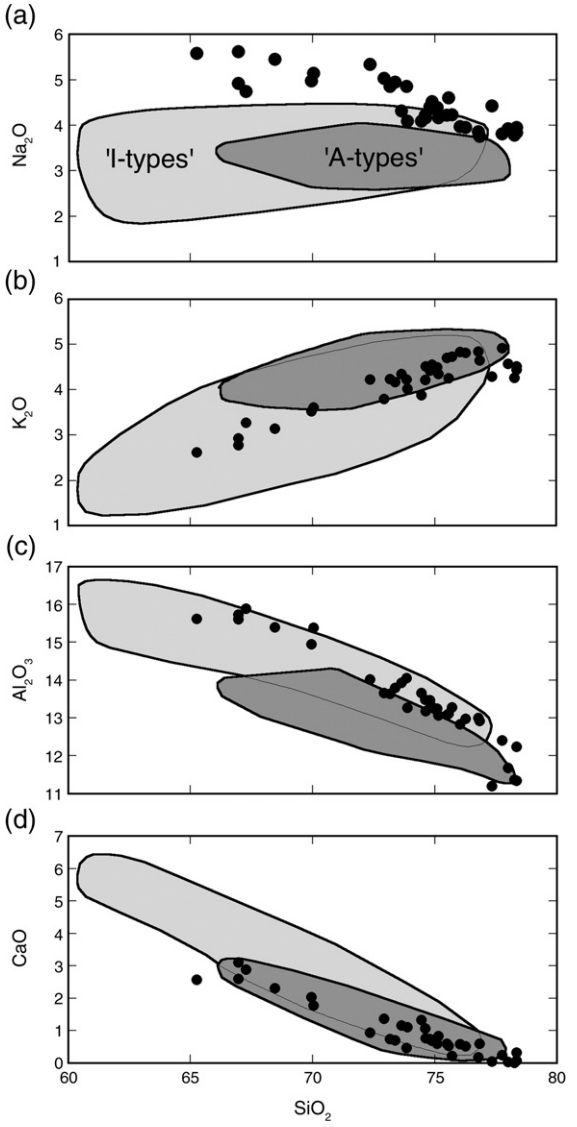

Fig. 2. Bulk-rock major element oxide data for samples from the Victoria Valley Batholith (filled black circles) illustrating variations in a) Na_2O, b) K_2O, c) Al_2O_3 and d) CaO with SiO_2. Fields for I-type and A-type magmas from the Lachlan Fold Belt are based on published figures and data from King et al. (2001) and references therein. Note the tendency for Na_2O to define the gently decreasing trend at the highest silica contents compared with the more dramatic drop in both K_2O and Al_2O_3 in these rocks.

than magmatic. Most calculated temperatures exceed 800 °C, similar to other Lachlan Fold Belt A-type granites and higher than I-types (e.g., King et al., 2001).

4.3. The oxidation state of the Victoria Valley magmas

The high iron contents of A-types have been related to their reduced oxidation state (e.g., Frost et al., 2001; King et al., 2001) and the Victoria Valley samples also have elevated total iron relative to MgO (Fig. 4b) compared with Lachlan Fold Belt I-type granites.

In contrast, where the opaque oxides in these rocks are euhedral, they display square cross-sections suggesting they crystallised as magnetite rather than ilmenite. Mineral analyses indicate that subsequent oxidation has converted many of these grains to hematite. Using unpublished FeO and Fe_2O_3 data (Atkinson, 1976; Hergt, 1983) and employing the approach of Kilinc et al. (1983) the fO_2 for the Victoria Valley rocks is estimated to lie around ΔNNO+2.5. Higher values for some of the peralkaline samples (some >6) are not used to infer the oxidation state of these magmas as the alkalies in excess of those "….required to charge balance the aluminium, help stabilise highly charged cations such as Fe^{3+} …" (Gwinn and Hess, 1989).

Despite evidence for the late-stage oxidation of magnetite grains, and therefore inevitable disturbance of the calculated fO_2 data, the values are consistent with the low FeOt/(FeOt+MgO) of the Victoria Valley bulk rock analyses on the discrimination diagram of Frost et al. (2001; Fig. 4c). On this figure,

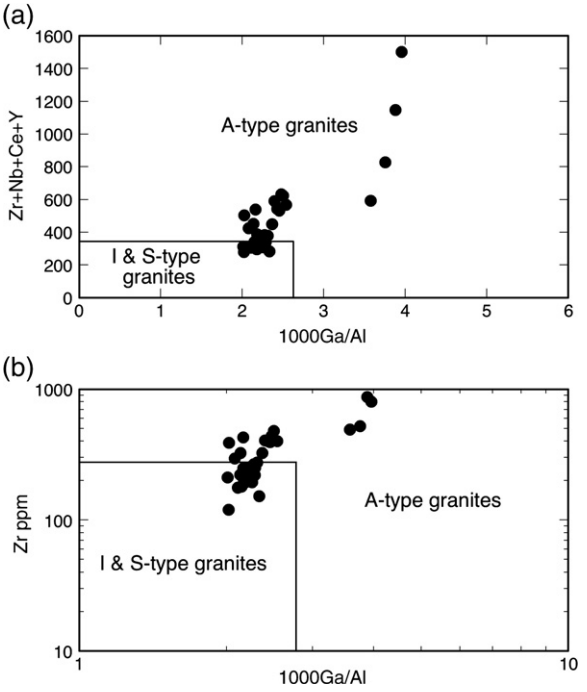

Fig. 3. Granite discrimination plots of a) Whalen et al. (1987) and b) Eby (1992) employing 10000 Ga/Al (note the log scale used on the axes of b). Panel a) indicates that, on the basis of the combined high field strength element contents of Zr and Nb, together with Ce and Y, the Victoria Valley granites plot into the A-type field. It is clear from b) that this relationship holds employing Zr alone. Note that four samples from the Mirranatwa Granite (VV11–VV14) plot at elevated Zr (+Nb+ Ce+Y).

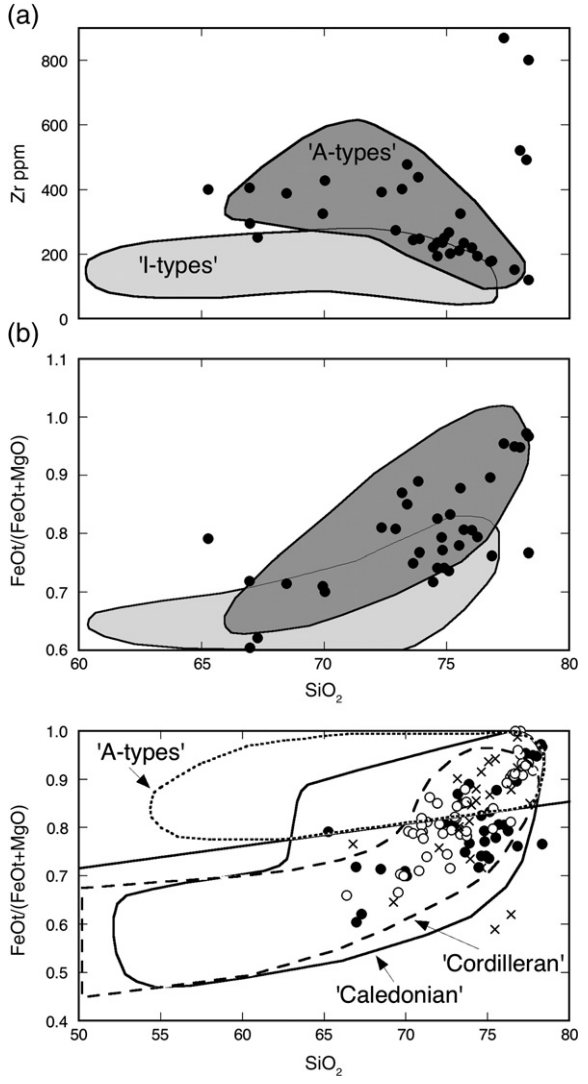

Fig. 4. Bulk-rock variations with SiO_2 of a) Zr content and both b) and c) the molecular proportion of total iron (as FeO) relative to total iron plus MgO for samples from the Victoria Valley Batholith. As noted in Fig. 2, four of the Mirranatwa Granite samples contain extraordinarily high Zr at ~77–78 wt.% SiO_2 (see text for discussion). Figure b) shows the Fe–Mg relationships of the Victoria Valley samples relative to Lachlan Fold Belt A-types and I-types. Figure c shows Australian A-type rocks relative to the 'ferroan–magnesian' discrimination boundary of Frost et al., 2001 where the discrimination line is defined as $FeO^{total}/(FeO^{total}+MgO)=0.486+0.0046\times wt.\%SiO_2$ (see text for discussion). Data sources as in Fig. 2 (LFB A-types, open circles) with additional results for the Padthaway Ridge A-types of the Adelaide Fold Belt (diagonal crosses, Turner et al., 1992).

the granites from the Victoria Valley are more closely related to the 'magnesian' fields of Cordilleran and Caledonian post-collisional granites than the A-type 'ferroan' rocks. Importantly, other A-types from the Lachlan Fold Belt (e.g., Gabo Island; Collins et al., 1982; Wangrah; King et al., 2001) as well as the older granites from the Adelaide Fold Belt (e.g., Padthaway Ridge; Turner et al., 1992) show the same 'magnesian' features as the Victoria Valley Batholith. Thus, although Australian A-types tend to display 'higher iron' relative to I-types (e.g., Fig. 4b), all are low in iron relative to magnesium, suggesting that they were comparatively more oxidised than 'typical' A-types employed in global datasets.

The results presented here highlight the difficulties in determining the fO_2 of slowly cooled magmas, particularly those emplaced at high levels in the crust where the exsolution of late-stage volatiles has occurred. We would argue that, at least in this example, mineral Fe–Mg relationships are not reliable indicators of magma oxidation states.

4.4. Sr, Nd and Hf isotope compositions of the Victoria Valley magmas

A large range in Rb/Sr and present-day $^{87}Sr/^{86}Sr$ ratios is preserved in whole-rocks sampled from across the batholith and representing all lithologies (Table 2). Seventeen samples yield an age estimate of 395.5+1.8/−8.7 Ma (95% confidence) with an initial $^{87}Sr/^{86}Sr$ ratio of around 0.7046 (Fig. 5), both of which are consistent with previous studies (e.g., Hergt, 1983).

In contrast with the Rb–Sr data, the Sm/Nd and present-day $^{143}Nd/^{144}Nd$ ratios show very little variation (Table 2), and the initial $^{143}Nd/^{144}Nd$ ratios calculated at an age of 396 Ma, yield an average of around 0.51220 (εNd+1.4).

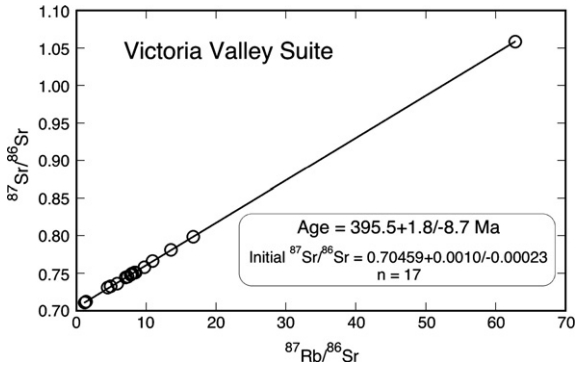

Fig. 5. Rb–Sr isochron employing seventeen samples from the Victoria Valley Batholith. The age estimate and uncertainties are quoted at the 95% confidence level and were calculated using the robust regression method of Isoplot/Ex version 3.0 (Ludwig, 2003). Samples from the three main lithologies and a rhyolite are included in the isochron. Two samples from the Mirranatwa Granite exhibiting elevated Zr plot away from the isochron at $^{87}Rb/^{86}Sr>100$ (not shown) and have not been included in the isochron calculation.

A somewhat unusual analytical complication was encountered in the Hf isotope analysis of the Victoria Valley zircons in that they possess extremely high Lu/Hf ratios with measured $^{176}Lu/^{177}Hf$ ratios of up to 0.012. In such cases up to 70% of the signal on mass 176 can be attributed to ^{176}Yb and ^{176}Lu interferences, and accurate peak stripping becomes problematic. In all of our analyses we use the improved Yb interference correction procedure described in Woodhead et al. (2004) but, nevertheless, we still observe a very minor correlation between corrected Hf-isotope ratio and measured Lu/Hf, even when radiogenic in-growth over 396 Ma is taken in to account (Fig. 6). This is most likely due to the inability of normal correction procedures to deal with interferences of such a size, which are an order of magnitude greater than those observed in typical zircons. This error, however, only results in a loss of accuracy ~3 times that of the analytical reproducibility for these run conditions. Based upon this, we would argue that the Victoria Valley zircons represent a single population with Fig. 6 constraining the initial Hf isotope ratio to around 0.28274 at 396 Ma (εHf+7.6), and suggest that the small spread of values to higher $^{176}Hf/^{177}Hf$ is largely an analytical artifact.

In order confirm the veracity of this estimate, several zircon grains were hand-picked from sample VV5 of the Bullawin Porphyry for digestion and purification of Hf prior to a solution ICPMS analysis which is free from any such interference concerns. The grains were ground in agate under alcohol and transferred to a teflon beaker. Here they were cleaned with 18 MΩ water and very dilute HCl, and dried. The zircon was then transferred to a Teflon pressure vessel and dissolved using HF and HNO_3 in oven set at 160 °C for 3 days, followed by evaporation and redigestion in the oven using 6 M HCl. No residue was observed in the final solution and the Hf was purified employing established column chemistry protocols (Woodhead and Hergt, 2005). A column blank run alongside this sample contained 6 pg Hf which is negligible relative to the estimated quantity of Hf extracted from the zircon (~256 ng). The sample solution was run twice and adjusted to a JMC475 value of 0.282160, based on four analyses of JMC475 throughout the analytical session. This yields present-day ratios of 0.282754 (±4) and 0.282755 (±5) for the zircon sample, with an initial ratio identical to that estimated from the laser ablation work, confirming the high initial $^{176}Hf/^{177}Hf$ of these magmas.

The low initial $^{87}Sr/^{86}Sr$ and high $^{143}Nd/^{144}Nd$ and $^{176}Hf/^{177}Hf$ are unexpected in granites derived from the partial melting of typical continental crust and imply derivation either involving mantle-derived magmas, or via the partial melting of juvenile crustal lithologies.

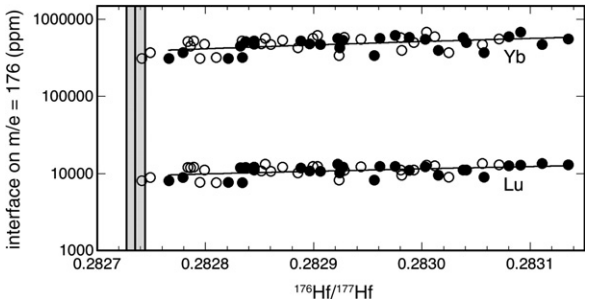

Fig. 6. An illustration of the subtle variation in the $^{176}Hf/^{177}Hf$ ratios of zircons measured from three samples from the Victoria Valley suite. This variation cannot be attributed to changes in the lithology, radiogenic in-growth, or drift in the instrument. Indeed sample VV11 from the Mirranatwa Granite is one of the samples preserving an unusually elevated Zr content and hydrothermal zircon morphologies, yet the Hf isotope compositions are indistinguishable from the two 'normal' samples. Instead, the correction procedures are unable to completely remove the effects of the unusually large isobaric interference on mass 176, derived from both ^{176}Yb and ^{176}Lu. Black symbols represent the data as measured (corrected for interferences) and open circles represent these data age-corrected to 396 Ma. We interpret the lower end of these arrays to best represent the initial $^{176}Hf/^{177}Hf$ ratio of the Victoria Valley magmas (i.e., ~0.28274), an inference confirmed by a single solution ICPMS analysis of a zircon from the Bullawin Porphyry (vertical band defines the isotope ratio and associated uncertainty; 2sd).

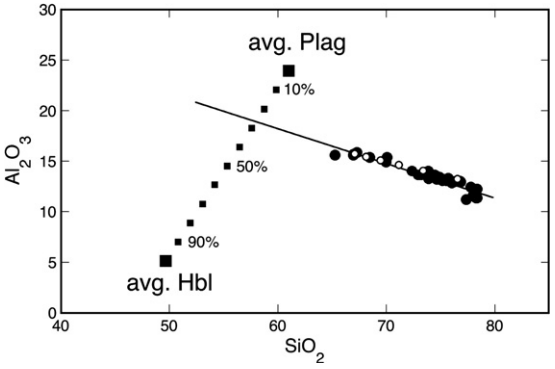

Fig. 7. Simple fractionational crystallisation model for the Victoria Valley Batholith. Average hornblende and plagioclase phenocryst compositions were determined from samples of the Bullawin Porphyry. Small black squares plot the composition of assemblages formed from different proportions of these phases. The black circles are the data for the Victoria Valley samples with a best-fit line projecting to an assemblage of approximately 30% hornblende and 70% plagioclase. The white circles are compositions based on the removal of this assemblage from an average Bullawin Porphyry composition. Between zero and 50% fractional crystallization of this kind of assemblage can account for most of the variation in the Victoria Valley magmas. Similar diagrams can be plotted for other elements, although those involving TiO_2 and FeO* require the addition of a small amount (<1%) an oxide phase to the fractionating assemblage.

5. Discussion

5.1. Within-suite variation

In terms of the major element variations, these appear to be consistent with fractional crystallisation of magmas such as those forming the Bullawin Porphyry (Atkinson, 1976; Hergt, 1983). The removal of an assemblage comprising plagioclase (~70%) and amphibole (~30%) with compositions similar to the phenocrysts in the Bullawin Porphyry can explain the decrease in CaO, Na_2O, Al_2O_3 and MgO with increasing K_2O and SiO_2, once some allowance is made for the progressive decrease in Ca in the plagioclase and Mg in the amphibole at higher silica contents (e.g., Fig. 7). In order to explain the decrease in TiO_2 and FeO (total), a small amount of Fe–Ti oxide removal is also required. The possibility that the Bullawin Porphyry represents a cumulate phase rather than a mafic magma has been excluded owing to the lack of cumulate textures, the moderate REE contents and negative Eu anomalies in VV1 to VV7 (Fig. 8).

Fig. 9 illustrates the mantle-normalised trace element abundances of the Victoria Valley samples. Several features are worth noting. First, as illustrated in Fig. 8, there is an overall coherence between the samples despite the large range in silica contents. The Bullawin Porphyry samples VV1 to VV7 are very similar in composition and, while sharing the same broad enrichment in elements to the left of Sr, and comparatively flat patterns to the right of Sr, these samples have smaller negative anomalies in Ba, Sr, P, Eu and Ti compared with most of the other rocks. The variation in element abundances in the Victoria Valley Granite samples is greater, but these rocks still define a tight

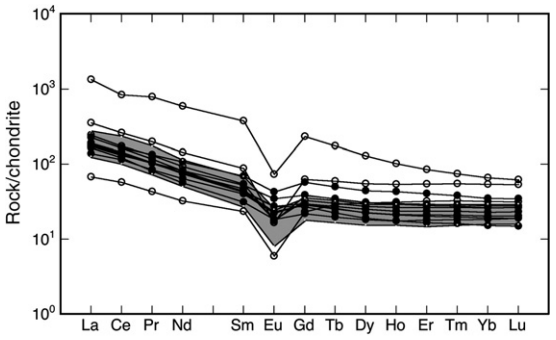

Fig. 8. Chondrite normalised plot of Victoria Valley Granite (shaded region), Mirranatwa Granite (open circles) and Bullawin Porphyry (filled circles) compositions. Normalising data are from Sun and McDonough (1989).

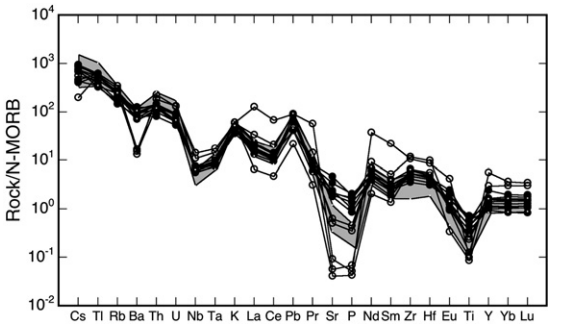

Fig. 9. Mantle normalised trace element compositions of samples from the Victoria Valley Granite (shaded region), Mirranatwa Granite (open circles) and Bullawin Porphyry (filled circles). NMORB normalising values are from Sun and McDonough (1989).

group and the relative enrichments and depletions are enhanced. In contrast, although patterns for two of the Mirranatwa Granite samples (VV9 and VV10) are very similar to the Victoria Valley Granites, three display erratic mantle normalised trace element patterns. The two patterns on Fig. 9 with highest LREE, Nb, Ta, Zr and Hf contents are VV11 and VV14, whereas VV12 has anomalously low REE contents. All three samples display striking depletions in Ba, Sr, and P relative to all other samples. The reasons for the unusual patterns in VV11, VV12 and VV14 compared with VV9, VV10, and the rest of the batholith are currently unknown, but may reflect some form of late-stage hydrothermal alteration (consistent with the morphology of the zircons extracted from VV11 for Hf isotope analysis).

In addition to the major element variations, and broad coherence in trace element signatures, all three phases of the batholith are co-linear on the Rb–Sr isochron, which argues against the operation of open-system processes such as AFC or mixing in generating the chemical variations now preserved. Two of the three unusual samples from the Mirranatwa Granite (VV11 and VV12) plot away from the main array, at unusually high Rb/Sr (>100, owing mainly to the low Sr contents illustrated in Fig. 9) and have been excluded from the isochron as the 'alteration'(?) appears to have disrupted their Rb/Sr and/or $^{87}Sr/^{86}Sr$ ratios. As the results for the remaining three Mirranatwa Granite samples VV9, VV10 and VV13 lie on the same isochron as the Bullawin Porphyry and the Victoria Valley Granite data, we conclude that all three magmatic groups are related by closed-system processes.

A lack of variation in the Nd and Hf isotopic compositions across the Victoria Valley suite is also consistent with closed-system fractional crystallisation of a single parent magma type.

5.2. The link between the peralkaline and more aluminous magmas

Together, the petrographic observations and elemental variations indicate that, although the Na_2O contents of Victoria Valley suite are unusually high, this is more extreme in the most mafic samples and values converge with more typical granite compositions at around 75% SiO_2. Consequently, the more felsic rocks of the Victoria Valley have Na_2O and K_2O contents similar to other Lachlan Fold Belt granites indicating that the peralkaline mineralogy observed in the Mirranatwa Granite is not a function of elevated Na_2O in these highly felsic magmas. Instead, the peralkaline mineralogy must reflect lower Al_2O_3 contents in these rocks (Fig. 2c) and/or additional processes.

As only one sample has a peralkaline bulk-rock composition, and the sodic pyroxenes and amphiboles appear to replace pre-existing hornblende, it is possible that late-stage subsolidus alteration has played an important role in producing the observed mineralogy of the Mirranatwa Granite. Given their shallow level of emplacement, the localised interaction between sodium-rich fluids (or fluid-rich silicate liquids ?) and parts of the Victoria Valley Granite might have generated the Mirranatwa peralkaline unit, with alteration even more severe if these also carried F (as suggested by the presence of fluorite). The late-stage hydration of pyroxene-bearing magmas to hornblende+biotite lithologies intruded as granites is well known from volcanic-intrusive complexes (e.g., conversion of clinopyroxene to hornblende). Although others have documented similar processes involving externally source fluids from regionally metamorphosed country rocks (e.g., Bucher and Frost, 2006) these fluids did not involve the mobilisation of sodium or zirconium and therefore would not produce the effects we observe. The high level of emplacement of the Victoria Valley Batholith (i.e., lack of regional metamorphism adjacent to the complex) and observation that some samples of the Mirranatwa Granite lie on the same Rb–Sr isochron as the other lithologies requires that the alteration was essentially synchronous with emplacement and that the fluids were magmatic (i.e., shared the same initial $^{87}Sr/^{86}Sr$ as the unaltered rocks). Consequently, studies concerning the alkali exchange between silicate melts and a coexisting volatile phase (e.g., Williams et al., 1997; Frank et al., 2003) and mobility of Zr (e.g., Rubin et al., 1989, 1993) are more likely to explain the phenomena observed here.

Importantly, at least in this case, the peralkaline and more aluminous magmas are closely related by fractional crystallisation and alteration processes. Debate surrounding whether or not to consider peralkaline A-types and more aluminous A-types as distinct groups or as members of the same (or similar) suite therefore requires the careful assessment of each specific case.

5.3. The source of the Victoria Valley magmas

The relatively low $^{87}Sr/^{86}Sr$ and high $^{143}Nd/^{144}Nd$ and $^{176}Hf/^{177}Hf$ initial ratios of the Victoria Valley suite suggest the involvement of mantle or juvenile mafic crust in their magmagenesis. The possibility that this unusual suite of magmas was derived via the partial melting of "..a source of basaltic composition, probably amphibolites…" was suggested by Chappell et al. (1988) and, given the geological history of this area, likely candidates include Cambrian greenstones (of mafic to intermediate composition) or other igneous rocks such as those represented by the Bushy Creek pluton.

A recent study of the 495 Ma Bushy Creek Granodiorite and related rocks (Whelan et al., in press) is particularly relevant to the origin of the Victoria Valley magmas. Data obtained from Bushy Creek lithologies and associated greenstones display elevated Na_2O contents, consistent with previous reports (e.g., Chappell et al., 1988). The main pluton displays aeromagnetic zonation, despite the similarities in bulk rock compositions, interpreted as indicating variations in the oxidation states of magmatic pulses.

Importantly, by calculating how the Sr, Nd and Hf isotope compositions for these 495 Ma old lithologies would have evolved by the time the Victoria Valley Batholith was emplaced, it is possible to compare the two magmatic groups directly. Fig. 10 shows the close match

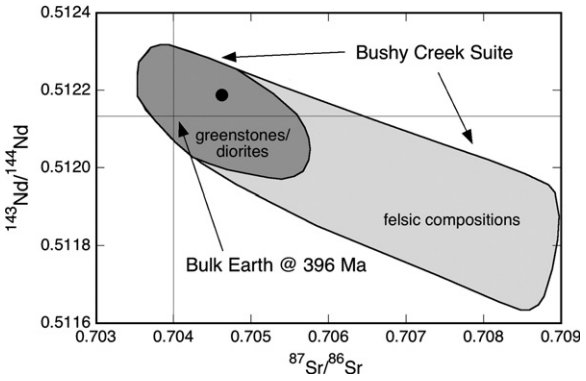

Fig. 10. $^{87}Sr/^{86}Sr$ vs $^{143}Nd/^{144}Nd$ isotope diagram illustrating the initial isotopic composition of the Victoria Valley magmas at the time of their emplacement (filled black circle). This is shown relative to Cambrian greenstones and diorites associated with the Bushy Creek pluton (corrected to this same age). Separate fields for the mafic and felsic Bushy Creek lithologies are from Whelan et al. (in press).

between the Sr and Nd isotopic composition of the greenstones and diorites associated with the Bushy Creek pluton and the Victoria Valley Batholith at 396 Ma. In addition the zircon Hf isotope data for Bushy Creek (average 0.28267) are also similar to the initial Hf isotope composition obtained from the Victoria Valley suite. The likelihood that the Bullawin Porphyry was derived from via partial melting of greenstones and diorites similar to those exposed in the vicinity of Bushy Creek is difficult to argue against. Importantly, the more felsic of these Late Cambrian lithologies tend to have higher $^{87}Sr/^{86}Sr$ and lower $^{143}Nd/^{144}Nd$ ratios making them less suitable as potential source rocks despite their lower melting temperatures. This supports the suggestion of White and Chappell (1988) that the source rocks for the Victoria Valley suite lie in the 'basaltic' basement that underlies the Grampians–Stavely Zone.

Although a source of heat and/or extension is required to trigger partial melting to generate magmas such as the Bullawin Porphyry, the extent to which either process took place remains unclear. The flat HREE patterns in the Victoria Valley rocks indicates that partial melting cannot have taken place at levels where garnet would be a stable residual phase, consistent with thinned crust.

Thus, we prefer a model that does not require the material involvement of mantle-derived magmas (e.g., as proposed by Turner et al., 1992; Turner and Foden, 1996 to explain the A-types of the Adelaide Fold Belt); *however*, this does not preclude such processes from explaining the *generation of the* Cambrian protoliths from which the Victoria Valley magmas were derived.

6. Conclusions

The western margin of the Lachlan Fold Belt is of particular interest given the increasing evidence that Lachlan Fold Belt magmatism in this region is superimposed upon underlying rocks of the Adelaide Fold Belt. Thus the granites of the Grampians–Stavely Zone preserve information relating to the temporal evolution of the continental crust at the overlapping margins of two fold belts, with important ramifications for the tectonic assembly of S.E. Australia, and models of crustal growth.

While the Delamerian age of the Bushy Creek pluton (485 Ma) clearly sets it apart from the Devonian granites, it is also intriguing as this demonstrates that, whatever the nature of the high sodium source region, it has been available since at least ~500 Ma, and appears to have yielded granitic magmas during two separate episodes of partial melting.

It is surprising that, despite their unusual compositions, and important location relative to two orogenic belts, no comprehensive study has previously been made of the Grampians–Stavely Zone granites. Granites with peralkaline mineralogy constitute part of the suite and appear to have been generated in the final stages of magmatism. This may have been caused by the reduction in Al_2O_3 relative to Na_2O and K_2O during fractional crystallisation in some rocks, although hydrothermal alteration involving magmatic fluids is required to explain the unusual trace element characteristics preserved in some samples of the Mirranatwa Granite. That all lithologies belong to a single suite is reinforced by the Rb–Sr isotope data acquired on samples from the compositional spectrum of the Victoria Valley suite that together preserve an age of $396+1.8/-8.7$ Ma. Consequently, peralkaline granites should not necessarily be considered to have a petrogenesis distinct from more aluminous magmas.

Similarities in certain major element features of the Victoria Valley suite and the Late Cambrian Bushy Creek pluton (e.g., high Na_2O and *possibly high* fO_2) suggest that these may have tapped the same source region at different times in the geological history of this region. Alternatively, as the match between the isotopic compositions of Sr, Nd and Hf of the Victoria Valley magmas at the time of their emplacement, and the Cambrian diorites of the Bushy Creek pluton recalculated to this time is remarkable, the partial melting of similar diorites in the basement beneath the Victoria Valley also provides a plausible model for the generation of these unusual magmas. This is analogous to a model proposed by Frost and Frost (1997) for the generation of reduced A-type magmas with rapakivi textures; however, in our case the oxidised nature of the Cambrian greenstones, diorites and granodiorites would explain the higher fO_2 of the partial melts derived from them, and the gap in time between formation of the protoliths and re-melting to generate the Victoria Valley magmas was around 100 Ma. Such an origin is consistent with the high Y/Nb and Yb/Ta (circa 2.5 and 3 respectively) of the Victoria Valley rocks, with such A-types thought to reflect regions influenced by continental margin or island arc processes (Eby, 1992).

Although likely to have been more oxidised than 'typical' A-types, we argue that the granites and rhyolites of the Victoria Valley Batholith preserve a number of petrographic and geochemical characteristics viewed as diagnostic for A-type granites and as such are classified here as an A-type suite. The increasing number of examples for which this appears to be the case suggests that low fO_2 should not be included as one of the distinguishing features of A-type magmas.

Acknowledgements

Initial inspiration for this work was provided by Chris Gray in 1983 and his energy and enthusiasm are warmly acknowledged. The final impetus for completing the analytical work some 20 years later, and writing this paper was provided by the IGCP-510 team! Roland Maas is thanked for his contributions to the generation of some of the isotope data, Bruce Chappell for the high quality of his XRF data and Alan Greig for his dedication to providing trace element results in time for submission of the revised version of the manuscript. The original text was substantially improved following constructive comments and suggestions by two anonymous reviewers.

References

Anderson, J.L., Bender, E.E., 1989. Nature and origin of Proterozoic A-type granitic magmatism in the southwestern United States of America. Lithos 23, 19–52.

Atkinson, P.L., 1976. Geology and geochemistry of the Victoria Valley Batholith, Grampians Ranges southeastern Australia. Unpublished BSc Honours thesis, La Trobe University.

Bucher, K., Frost, B.R., 2006. Fluid transfer in high-grade metamorphic terrains intruded by anorogenic granites: the Thor Range, Antarctica. Journal of Petrology 47, 567–593.

Cayley, R.A., Taylor, D.H., 1997. Grampians special map area geological report. Geological Survey of Victoria Report 107, 150 pp.

Chappell, B.W., White, A.J.R., 1992. I- and S-type granites in the Lachlan Fold Belt. Transactions of the Royal Society of Edinburgh. Earth Sciences 83, 1–26.

Chappell, B.W., White, A.J.R., Hine, R., 1988. Granite provinces and basement terranes in the Lachlan Fold Belt, southeastern Australia. Australian Journal of Earth Sciences 35, 505–521.

Chappell, B.W., English, P.M., King, P.L., White, A.J.R., Wyborn, D., 1991. Granites and related rocks of the Lachlan Fold Belt (1:1 250 000 Scale Map). Bureau of Mineral Resources, Canberra.

Clemens, J.D., Holloway, J.R., White, A.J.R., 1986. Origin of an A-type granite: experimental constraints. American Mineralogist 71, 317–324.

Collins, W.J., Beams, S.D., White, A.J.R., Chappell, B.W., 1982. Nature and origin of A-type granites with particular reference to southeastern Australia. Contributions to Mineralogy and Petrology 80, 189–200.

Creaser, R.A., Price, R.C., Wormald, R.J., 1991. A-type granites revisited: assessment of a residual-source model. Geology 19, 163–166.

Dall'Agnol, R., Teixeira, N.P., Rämo, T., Moura, C.A.V., Macambira, M.J.B., de Oliveira, D.C., 2005. Petrogenesis of the Paleoproterozoic rapakivi A-type granites of the Archean Carajás metallogenic province, Brazil. Lithos 80, 101–129.

Eby, G.N., 1992. Chemical subdivision of the A-type granitoids: petrogenetic and tectonic implications. Geology 20, 641–644.

Eggins, S.M., Woodhead, J.D., Kinsley, L.P.J., Mortimer, G.E., Sylvester, P., McCulloch, M.T., Hergt, J.M., Handler, M.R., 1997. A simple method for the precise determination of >40 trace elements in geological samples by ICPMS using enriched isotope internal standardisation. Chemical Geology 134, 311–326.

Frank, M.R., Candela, P.A., Piccoli, P.M., 2003. Alkali exchange equilibria between a silicate melt and coexisting magmatic volatile phase: an experimental study at 800 °C and 100 MPa. Geochimica et Cosmochimica Acta 67, 1415–1427.

Frost, C.D., Frost, B.R., 1997. Reduced rapakivi-type granites: the tholeiite connection. Geology 25, 647–650.

Frost, B.R., Barnes, C.G., Collins, W.J., Arculus, R.J., Ellis, D.J., Frost, C.D., 2001. A geochemical classification for granitic rocks. Journal of Petrology 42, 2033–2048.

Gwinn, R., Hess, P.C., 1989. Iron and titanium solution properties in peraluminous and peralkaline rhyolitic liquids. Contributions to Mineralogy Petrology 101, 326–338.

Hergt, J.M., 1983. The igneous rocks of the Grampians, southeastern Australia: a petrographic, geochemical and isotopic study. Unpublished BSc Honours thesis, La Trobe University.

Hergt, J.M., Chappell, B.W., McCulloch, M.T., McDougall, I., Chivas, A.R., 1989. Geochemical and isotopic constraints on the origin of the Jurassic Dolerites of Tasmania. Journal of Petrology 30 (4), 841–883.

Kilinc, A., Carmichael, I.S.E., Rivers, M.L., Sack, R.O., 1983. The ferric–ferrous ratio in natural silicate liquids equilibrated in air. Contributions to Mineralogy and Petrology 83, 136–140.

King, P.L., White, A.J.R., Chappell, B.W., 1997. Characterization and origin of aluminous A type granites of the Lachlan Fold Belt, southeastern Australia. Journal of Petrology 36, 371–391.

King, P.L., Chappell, B.W., Allen, C.M., White, A.J.R., 2001. Are A-type granites the high-temperature felsic granites? Evidence from fractionated granites of the Wangrah Suite. Australian Journal of Earth Sciences 48, 501–514.

Loiselle, M.C., Wones, D.R., 1979. Characteristics and origin of anorogenic granites. Geological Society of America Abstracts 11, 468.

Ludwig, K.R., 2003. Isoplot/Ex version 3.0, A Geochronological Toolkit for Microsoft Excel. Berkeley Geochronology Center Special Publication, vol. 4.

Makishima, A., Nakamura, E., Nakano, T., 1999. Determination of zirconium, niobium, hafnium and tantalum at ng g^{-1} levels in geological materials by direct nebulisation of sample HF solution into FI-ICP-MS. Geostandards Newsletter: The Journal of Geostandards and Geoanalysis 23, 7–20.

Qui, J.S., Wang, D.Z., McInnes, B.I.A., Jiang, S.Y., Wang, R.C., Kanisawa, S., 2004. Two subgroups of A-type granites in the coastal area of Zhejiang and Fujian Provinces, SE China: age and geochemical constraints on their petrogenesis. Transactions of the Royal Society of Edinburgh. Earth Sciences 95, 227–236.

Reid, J.E., Horn, I., Longerich, H.P., Forsythe, L., Jenner, G.A., 1999. Determination of Zr and Hf in a flux-free fusion of whole rock samples using laser ablation inductively coupled plasma-mass spectrometry (LA-ICP-MS) with isotope dilution calibration. Geostandards Newsletter: The Journal of Geostandards and Geoanalysis 23, 149–155.

Richards, R., Singleton, O.P., 1981. Palaeozoic Victoria Australia: igneous rocks, ages and their interpretation. Journal of the Geological Society of Australia 28, 395–421.

Robinson, P., Townsend, A.T., Yu, Z., Münker, C., 1999. Determination of scandium, yttrium and rare earth elements in rocks by high resolution inductively coupled plasma-mass spectrometry. Geostandards Newsletter: The Journal of Geostandards and Geoanalysis 23, 31–46.

Rubin, J.N., Henry, C.D., Price, J.G., 1989. Hydrothermal zircons and zircon overgrowths, Sierra Blanca Peaks, Texas. American Mineralogist 72, 865–869.

Rubin, J.N., Henry, C.D., Price, J.G., 1993. The mobility of zirconium and other "immobile" elements during hydrothermal alteration. Chemical Geology 110, 29–47.

Simpson, C., Rocklands Volcanics Group, 1997. In: Cayley, R.A., Taylor, D.H. (Eds.), Grampians Special Map Area Geological Report. Geological Survey of Victoria Report, vol. 107, pp. 61–66.

Spencer-Jones, D., 1965. The geology and structure of the Grampians area western Victoria. Geological Survey of Victoria Memoir 25, 92 pp.

Stuart-Smith, P.G., Black, L., 1999. Willaura Sheet 7422, Victoria 1:100 000 map geological report. Australian Geological Survey Organisation Record 1999/38.

Sun, S.S., McDonough, W.F., 1989. Chemical and isotopic systematics of oceanic basalts: implications for mantle composition and processes. In: Sauders, A.D., Norry, M.J. (Eds.), Magmatism in the Ocean Basins. Geological Society of London Special Paper, vol. 42, pp. 313–345.

Turner, S.P., Foden, J.D., 1996. Magma mingling in late-Delamerian A-type granites at Mannum, South Australia. Mineralogy and Petrology 56, 147–169.

Turner, S.P., Foden, J.D., Morrison, R.S., 1992. Derivation of an A-type magma by fractionation of basaltic magma: an example from the Padthaway Ridge South Australia. Lithos 28, 151–179.

Vandenberg, A.H.M., 1978. The Tasman Fold Belt system in Victoria. Tectonophysics 48, 267–297.

Watson, E.B., Harrison, T.M., 1983. Zircon saturation revisited: temperature and composition effects in a variety of crustal magma types. Earth and Planetary Science Letters 64, 295–304.

Whalen, J.B., Currie, K.L., Chappell, B.W., 1987. A-type granites: geochemical characteristics, discrimination and petrogenesis. Contributions to Mineralogy and Petrology 95, 407–419.

Whelan, J., Hergt, J., Woodhead, J., in press. The granite–greenstone connection in Western Victoria: an example from the Bushy Creek igneous complex. Australian Journal of Earth Sciences 54.

White, A.J.R., Chappell, B.W., 1988. Granites. In: Douglas, J.G., Ferguson, J.A. (Eds.), Geology of Victoria. Geological Society of Australia, Victoria Division, Melbourne, pp. 427–439.

Williams, T.J., Candela, P.A., Piccoli, P.M., 1997. Hydrogen–alkali exchange between silicate melts and two-phase aqueous mixtures: an experimental investigation. Contributions to Mineralogy and Petrology 128, 114–126.

Woodhead, J.D., Hergt, J.M., 2005. A preliminary appraisal of seven natural zircon reference materials for in situ Hf-isotope analysis. Geostandards and Geoanalytical Research 29, 183–195.

Woodhead, J.D., Hergt, J.M., Shelley, M., Eggins, S., Kemp, R., 2004. Zircon Hf-isotope analysis with an excimer laser, depth profiling, ablation of complex geometries, and concomitant age estimation. Chemical Geology 209, 121–135.

Wormald, R.J., Price, R.C., Kemp, A.I.S., 2004. Geochemistry and Rb–Sr geochronology of the alkaline–peralkaline Narraburra Complex, central southern New South Wales; tectonic significance of Late Devonian granitic magmatism in the Lachlan Fold Belt. Australian Journal of Earth Sciences 51, 369–384.